

A FIFTH-ORDER ACCURATE WEIGHTED ENN DIFFERENCE SCHEME AND ITS APPLICATIONS^{*1)}

Yi-qing Shen

(*Department of Mathematics, Yunnan University, Kunming 650091, China*)

Ru-quan Wang

(*ICMSEC, Academy of Mathematics and Systems Sciences, Chinese Academy of Sciences, Beijing 100080, China*)

Hong-zhi Liao

(*Department of Mathematics, Yunnan University, Kunming 650091, China*)

Abstract

In this paper, we have constructed a high accurate difference scheme based on the ENN scheme [1]. The new scheme has 5th-order accuracy in smooth regions and can keep the essentially non-oscillatory property.

Key words: ENN scheme, WENO scheme, Shock-boundary-layer interaction.

1. Introduction

In the paper [1], where Zhang Hanxin et al. presented the nonoscillatory 3rd-order ENN difference scheme. The idea of ENN scheme is to compare the 1st-order difference and 2nd-order difference to attain 3rd-order accurate scheme and to avoid spurious oscillations near shocks. However the ENN scheme has certain drawbacks. One problem is only 3rd-order accuracy even in the very smooth regions. Another is to use a lot of logical statements which affect the convergence rate and the efficiency of parallel computing.

Recently, G.-S. Jiang and C.-W. Shu developed a 5th-order weighted ENO scheme [2] based on the third-order accurate difference scheme in the flux form. We found that the third-order accurate ENO scheme given in [2] with $r=3$ is the same as the ENN scheme without the limiters. Naturally, the ENN scheme would be expanded to 5th-order accurate scheme by using the idea of deriving the 5th-order WENO difference scheme.

In this paper, we have constructed the higher accuracy difference scheme based on the ENN scheme. The new scheme has 5th-order accuracy in smooth regions and can keep the essentially non-oscillatory property.

We tested the new scheme's accuracy by using a linear initial problem and tested its non-oscillatory property by using a nonlinear initial problem. At last, we applied the new scheme to compute the problem of shock-boundary-layer interaction. Numerical results showed that the new scheme is efficient.

2. ENN Scheme and Several High Order Accuracy Central Schemes

Consider a scalar conservative hyperbolic equation

$$\frac{\partial u}{\partial t} + \frac{\partial f(u)}{\partial x} = 0 \quad (1)$$

* Received December 24, 1997.

¹⁾This work was supported by the National Natural Science Foundation of China under grant NO.19582007 and The Key Laboratory of Scientific/Engineering Computing.

where f is a flux function and can be splitted into two parts, i.e. $f(u) = f^+(u) + f^-(u)$ and $df^+(u)/du \geq 0$ and $df^-(u)/du \leq 0$. In this paper we define $f^\pm(u) = \frac{1}{2}(f(u) \pm \alpha u)$ and $\alpha = \max|f'(u)|$ for one-dimensional equation. The semi-discrete conservative difference scheme can be written as follows

$$\frac{du_j}{dt} + \frac{(h_{j+\frac{1}{2}} - h_{j-\frac{1}{2}})}{\Delta x} = 0 \tag{2}$$

where the numerical flux $h_{j+\frac{1}{2}} = h_{j+\frac{1}{2}}^+ + h_{j+\frac{1}{2}}^-$.

(1) The ENN scheme[1]

$$h_{j+\frac{1}{2}}^+ = \begin{cases} f_j^+ + \frac{1}{2}\Delta f_{j+\frac{1}{2}}^+ - \frac{1}{6}ms(D_j^+, D_{j+1}^+) & \text{if } |\Delta f_{j+\frac{1}{2}}^+| \leq |\Delta f_{j-\frac{1}{2}}^+| \\ f_j^+ + \frac{1}{2}\Delta f_{j-\frac{1}{2}}^+ + \frac{1}{3}ms(D_j^+, D_{j-1}^+) & \text{if } |\Delta f_{j+\frac{1}{2}}^+| > |\Delta f_{j-\frac{1}{2}}^+| \end{cases} \tag{3}$$

$$h_{j+\frac{1}{2}}^- = \begin{cases} f_{j+1}^- - \frac{1}{2}\Delta f_{j+\frac{3}{2}}^- + \frac{1}{3}ms(D_{j+1}^-, D_{j+2}^-) & \text{if } |\Delta f_{j+\frac{3}{2}}^-| \leq |\Delta f_{j+\frac{1}{2}}^-| \\ f_{j+1}^- - \frac{1}{2}\Delta f_{j+\frac{1}{2}}^- - \frac{1}{6}ms(D_j^-, D_{j+1}^-) & \text{if } |\Delta f_{j+\frac{3}{2}}^-| > |\Delta f_{j+\frac{1}{2}}^-| \end{cases} \tag{4}$$

where $D_j = \Delta f_{j+\frac{1}{2}} - \Delta f_{j-\frac{1}{2}}$ and the $ms(a,b)$ is defined below

$$ms(a,b) = \begin{cases} a & |a| \leq |b| \\ b & |a| > |b| \end{cases} \tag{5}$$

(2) 4th-order accurate central schemes [3]

$$h_{j+\frac{1}{2}}^+ = f_j^+ + \frac{1}{2}\Delta f_{j+\frac{1}{2}}^+ - \frac{1}{12}D_j^+ - \frac{1}{12}D_{j+1}^+ \tag{6}$$

$$h_{j+\frac{1}{2}}^+ = f_j^+ + \frac{1}{2}\Delta f_{j-\frac{1}{2}}^+ + \frac{1}{4}D_j^+ + \frac{1}{12}D_{j-1}^+ \tag{7}$$

$$h_{j+\frac{1}{2}}^- = f_{j+1}^- - \frac{1}{2}\Delta f_{j+\frac{3}{2}}^- + \frac{1}{4}D_{j+1}^- + \frac{1}{12}D_{j+2}^- \tag{8}$$

$$h_{j+\frac{1}{2}}^- = f_{j+1}^- - \frac{1}{2}\Delta f_{j+\frac{1}{2}}^- - \frac{1}{12}D_{j+1}^- - \frac{1}{12}D_j^- \tag{9}$$

(3) 5-order accurate central scheme

$$h_{j+\frac{1}{2}}^+ = f_j^+ + \frac{3}{5} \times (\frac{1}{2}\Delta f_{j+\frac{1}{2}}^+ - \frac{1}{12}D_j^+ - \frac{1}{12}D_{j+1}^+) + \frac{2}{5} \times (\frac{1}{2}\Delta f_{j-\frac{1}{2}}^+ + \frac{1}{4}D_j^+ + \frac{1}{12}D_{j-1}^+) \tag{10}$$

$$h_{j+\frac{1}{2}}^- = f_{j+1}^- + \frac{2}{5} \times (-\frac{1}{2}\Delta f_{j+\frac{3}{2}}^- + \frac{1}{4}D_{j+1}^- + \frac{1}{12}D_{j+2}^-) + \frac{3}{5} \times (-\frac{1}{2}\Delta f_{j+\frac{1}{2}}^- - \frac{1}{12}D_{j+1}^- - \frac{1}{12}D_j^-) \tag{11}$$

3. Numerical Method

For simplicity, we show only the positive part of the splitted flux, and the negative part of the splitted flux are symmetric with respect to $x_{j+\frac{1}{2}}$.

From above equations, it can be seen that the combinal coefficients in (8) from (3) are

$$C_1^1 = \frac{1}{2}, C_2^1 = \frac{1}{2};$$

the combinal coefficients in (9) from (4) are

$$C_1^2 = \frac{3}{4}, C_2^2 = \frac{1}{4};$$

and in (12) from (8) & (9),the coefficients are

$$C_1 = \frac{3}{5}, C_2 = \frac{2}{5}.$$

(1) 4th-order weighted scheme

First, we weight (3) to obtain two 4th-order accurate numerical fluxes:

$$h_{j+\frac{1}{2}}^{1+} = f_j^+ + \frac{1}{2}\Delta f_{j+\frac{1}{2}}^+ - \frac{1}{6}(\omega_1^+ D_j^+ + \omega_2^+ D_{j+1}^+) \tag{14}$$

$$h_{j+\frac{1}{2}}^{2+} = f_j^+ + \frac{1}{2}\Delta f_{j-\frac{1}{2}}^+ + \frac{1}{3}(\omega_3^+ D_j^+ + \omega_4^+ D_{j-1}^+) \tag{15}$$

where

$$\omega_1^+ = \frac{\alpha_1}{\alpha_1 + \alpha_2}, \omega_2^+ = \frac{\alpha_2}{\alpha_1 + \alpha_2}, \omega_3^+ = \frac{\alpha_3}{\alpha_3 + \alpha_4}, \omega_4^+ = \frac{\alpha_4}{\alpha_3 + \alpha_4}.$$

$$\alpha_1 = \frac{C_1^1}{(\varepsilon + W_1)}, \alpha_2 = \frac{C_2^1}{(\varepsilon + W_2)}, \alpha_3 = \frac{C_1^2}{(\varepsilon + W_3)}, \alpha_4 = \frac{C_2^2}{(\varepsilon + W_4)}, \tag{16}$$

Based on the idea of the ENN scheme, we can obtain the 4th-order non-oscillatory scheme:

$$h_{j+\frac{1}{2}}^{4+} = \begin{cases} f_j^+ + \frac{1}{2}\Delta f_{j+\frac{1}{2}}^+ - \frac{1}{6}(\omega_1^+ D_j^+ + \omega_2^+ D_{j+1}^+) & \text{if } |\Delta f_{j+\frac{1}{2}}^+| \leq |\Delta f_{j-\frac{1}{2}}^+| \\ f_j^+ + \frac{1}{2}\Delta f_{j-\frac{1}{2}}^+ + \frac{1}{3}(\omega_3^+ D_j^+ + \omega_4^+ D_{j-1}^+) & \text{if } |\Delta f_{j+\frac{1}{2}}^+| > |\Delta f_{j-\frac{1}{2}}^+| \end{cases} \tag{17}$$

Through theoretical analysis and numerical result, the scheme (17) is 4th-order accurate in smooth regions, but only 3th-order in critical points.

The variables $W_k(k = 1, \dots, 4)$ will be discussed in section 4.

(2) 5th-order weighted scheme

We suppose that (14) and (15) are two 4th-order numerical fluxes, then we construct the 5th-order accurate scheme as follows:

$$h_{j+\frac{1}{2}}^+ = \Omega_1^+ h_{j+\frac{1}{2}}^{1+} + \Omega_2^+ h_{j+\frac{1}{2}}^{2+} \tag{18}$$

where

$$\Omega_1^+ = \frac{\beta_1}{\beta_1 + \beta_2}, \Omega_2^+ = \frac{\beta_2}{\beta_1 + \beta_2},$$

$$\beta_1 = \frac{C_1}{(\varepsilon + W_5^1)}, \beta_2 = \frac{C_2}{(\varepsilon + W_5^2)}, \tag{19}$$

The variables $W_5^k(k = 1, 2)$ will be discussed in section 4.

4. The Relation between the Weighted Functions and the Accuracy of Scheme

To achieve essentially non-oscillatory property, we require the scheme (18) approaches to the scheme (17) near shocks, on the other hand, we require the scheme (18) approaches to 5th-order accurate scheme (12) in smooth regions. Therefore, the weights must assure that only one flux is played into in discontinuous regions, and all fluxes go into effect in smooth regions.

We suppose $h_{j+\frac{1}{2}}^{n,1}$ and $h_{j+\frac{1}{2}}^{n,2}$ are two n th-order accurate flux functions, $h_{j+\frac{1}{2}}^{n+1}$ is a $(n+1)$ th order accurate flux function, which is expressed through the following relation

$$h_{j+\frac{1}{2}}^{n+1} = C_1 h_{j+\frac{1}{2}}^{n,1} + C_2 h_{j+\frac{1}{2}}^{n,2}, C_1, C_2 > 0, C_1 + C_2 = 1,$$

where, we require $\omega_1, \omega_2 > 0, \omega_1 + \omega_2 = 1$, and

$$\sum_{i=1}^2 \omega_i h_{j+\frac{1}{2}}^{n,i} = h_{j+\frac{1}{2}}^{n+1} + \sum_{i=1}^2 (\omega_i - C_i) (h_{j+\frac{1}{2}}^{n,i} - h_{j+\frac{1}{2}}^{n+1}) \tag{20}$$

If ω_i satisfies

$$\omega_i = C_i + O(h) \tag{21}$$

then the convex combination $\sum_{i=1}^2 \omega_i h_{j+\frac{1}{2}}^{n,i}$ is the $(n+1)$ th order accurate flux function. Of course, if $\omega_i = C_i + O(h^l), l > 1$, the scheme is more approximate to the $(n+1)$ th order scheme.

In the paper [2], authors presented a smoothness measurement :

$$IS_k = \sum_{i=1}^{r-1} \int_{x_{j-\frac{1}{2}}}^{x_{j+\frac{1}{2}}} h^{2l-1} (q_k^{(l)})^2 dx, k = 0, \dots, r-1 \tag{22}$$

where $q_k(x)$ is the interpolation polynomial on the stencil $(x_{j+k-r+1}, \dots, x_{j+k})$, $q_k^{(l)}$ is the l^{th} derivative of $q_k(x)$.

For $r=3$, the (22) gives

$$\begin{aligned} IS_0 &= \frac{13}{12}(f_{j-2} - 2f_{j-1} + f_j)^2 + \frac{1}{4}(f_{j-2} - 4f_{j-1} + 3f_j)^2 \\ IS_1 &= \frac{13}{12}(f_{j-1} - 2f_j + f_{j+1})^2 + \frac{1}{4}(f_{j-1} - f_{j+1})^2 \\ IS_2 &= \frac{13}{12}(f_j - 2f_{j+1} + f_{j+2})^2 + \frac{1}{4}(3f_j - 4f_{j+1} + f_{j+2})^2 \end{aligned} \tag{23}$$

In smooth regions, Taylor expansions of (23) give, respectively

$$\begin{aligned} IS_0 &= \frac{13}{12}(f'' h^2 - f''' h^3)^2 + \frac{1}{4}(2f' h - \frac{2}{3}f''' h^3)^2 + O(h^6) \\ IS_1 &= \frac{13}{12}(f'' h^2)^2 + \frac{1}{4}(2f' h + \frac{1}{3}f''' h^3)^2 + O(h^6) \\ IS_2 &= \frac{13}{12}(f'' h^2 + f''' h^3)^2 + \frac{1}{4}(2f' h - \frac{2}{3}f''' h^3)^2 + O(h^6) \end{aligned} \tag{24}$$

If $f' \neq 0$, then

$$IS_k = (f' h)^2 (1 + O(h^2)), k = 0, 1, 2. \tag{25}$$

When $f' = 0$, then

$$IS_k = \frac{13}{12}(f'' h^2)^2 (1 + O(h)), k = 0, 1, 2 \tag{26}$$

Therefore, in (16), we take

$$W_1 = IS_1, W_2 = IS_2, W_3 = IS_1, W_4 = IS_0 \tag{27}$$

and in (19), we take

$$W_5^1 = IS_2, W_5^2 = IS_0 \tag{28}$$

these variables will satisfy condition (21).

In other way, we can find new weight functions through the linear extrapolating by using the 1st-order differences $\Delta f_{j-\frac{3}{2}}, \Delta f_{j-\frac{1}{2}}, \text{ and } \Delta f_{j+\frac{1}{2}}, \Delta f_{j+\frac{3}{2}}$, i.e. in (19) take

$$W_5^1 = \frac{1}{2}(3\Delta f_{j+\frac{1}{2}}^+ - \Delta f_{j+\frac{3}{2}}^+)^2, W_5^2 = \frac{1}{2}(3\Delta f_{j-\frac{1}{2}}^+ - \Delta f_{j-\frac{3}{2}}^+)^2 \tag{29}$$

In smooth regions, Taylor expansions of (29) give

$$\begin{aligned} W_5^1 &= (f' h - \frac{1}{2} f''' h^3 + O(h^4))^2 \\ W_5^2 &= (f' h - \frac{1}{2} f''' h^3 + O(h^4))^2 \end{aligned} \tag{30}$$

If $f' \neq 0$, then

$$W_5^k = (f')^2 h^2 (1 + O(h^2)), k = 0, 1, \tag{31}$$

When $f' = 0$, then

$$W_5^k = \frac{1}{4} (f''')^2 h^6 (1 + O(h)), k = 0, 1 \tag{32}$$

So they can also satisfy the condition (21) and have the same accuracy.

Variable ε is a positive real number which is introduced to avoid the denominator to become zero, in this paper, $\varepsilon = 10^{-6}$.

5. Numerical Examples

(1) the linear initial problem

$$\begin{aligned} u_t + u_x &= 0, -1 \leq x \leq 1 \\ u(x, 0) &= u_0(x) \quad \textit{periodic}. \end{aligned} \tag{33}$$

In Table 1, we show the errors of these schemes at $t=1$ for the initial condition $u_0(x) = \sin(\pi x)$.

In Table 2, we show the errors of these schemes at $t=1$ for the initial condition $u_0(x) = \sin^4(\pi x)$.

(2) the nonlinear initial problem

$$\begin{aligned} \frac{\partial u}{\partial t} + \frac{\partial(\frac{u^2}{2})}{\partial x} &= 0, \quad 0 \leq x \leq 2\pi \\ u(x, 0) &= 0.3 + 0.7\sin x, \quad 0 \leq x \leq 2\pi \end{aligned} \tag{34}$$

The numerical results can be seen in fig. 1 with $N=40$ and fig. 2 with $N=80$ for $t = 2$.

(3) the nonlinear Burgers equation

$$\begin{aligned} \frac{\partial u}{\partial t} + u \frac{\partial u}{\partial x} &= \frac{1}{Re} \frac{\partial^2 u}{\partial x^2} \\ u(-1, t) &= 1, u(1, t) = 1, u(x, 0) = 0, -1 < x < 1. \end{aligned} \tag{35}$$

We computed the steady solution of (35) with $Re = 1000$, in Table 3, given the convergent times and errors of several schemes, where convergent criterion is:

$$\frac{1}{N} \sum_{i=1}^N |u_i^{n+1} - u_i^n| / \Delta t \leq 0.5 \times 10^{-3}$$

Table 1: Accuracy on $u_t + u_x = 0$, with $u_0(x) = \sin(\pi x)$.

| Method | N | $L_\infty error$ | $L_\infty order$ | $L_1 error$ | $L_1 order$ |
|--------|-----|------------------|------------------|-------------|-------------|
| ENN | 10 | 6.048e-2 | — | 3.753e-2 | — |
| | 20 | 8.606e-3 | 2.813 | 4.917e-3 | 2.932 |
| | 40 | 1.076e-3 | 3.000 | 6.307e-4 | 2.963 |
| | 80 | 1.353e-4 | 2.991 | 7.977e-5 | 2.983 |
| | 160 | 1.690e-5 | 3.001 | 1.003e-5 | 2.992 |
| | 320 | 2.094e-6 | 3.013 | 1.258e-6 | 2.995 |
| WENN-5 | 10 | 1.763e-2 | — | 1.005e-2 | — |
| | 20 | 8.908e-4 | 4.307 | 4.323e-4 | 4.539 |
| | 40 | 2.711e-5 | 5.038 | 1.283e-5 | 5.074 |
| | 80 | 8.733e-7 | 4.956 | 3.950e-7 | 5.022 |
| | 160 | 2.549e-8 | 5.099 | 1.238e-8 | 4.996 |
| | 320 | 7.270e-10 | 5.132 | 3.872e-10 | 4.998 |
| WENO-5 | 10 | 2.958e-2 | — | 1.591e-2 | — |
| | 20 | 1.455e-3 | 4.345 | 7.388e-4 | 4.429 |
| | 40 | 4.591e-5 | 4.986 | 2.221e-5 | 5.056 |
| | 80 | 1.475e-6 | 4.960 | 6.904e-7 | 5.008 |
| | 160 | 4.359e-8 | 5.081 | 2.166e-8 | 4.994 |
| | 320 | 1.277e-9 | 5.093 | 6.774e-10 | 4.998 |

Table 2: Accuracy on $u_t + u_x = 0$, with $u_0(x) = \sin^4(\pi x)$.

| Method | N | $L_\infty error$ | $L_\infty order$ | $L_1 error$ | $L_1 order$ |
|--------|-----|------------------|------------------|-------------|-------------|
| ENN | 10 | 3.511e-1 | — | 2.464e-1 | — |
| | 20 | 7.458e-2 | 2.235 | 3.821e-2 | 2.689 |
| | 40 | 3.429e-2 | 1.121 | 1.454e-2 | 1.394 |
| | 80 | 7.545e-3 | 2.184 | 2.969e-3 | 2.292 |
| | 160 | 1.410e-3 | 2.420 | 4.424e-4 | 2.747 |
| | 320 | 3.351e-4 | 2.073 | 8.270e-5 | 2.419 |
| WENN-5 | 10 | 2.823e-1 | — | 1.801e-1 | — |
| | 20 | 8.042e-2 | 1.812 | 4.159e-2 | 2.115 |
| | 40 | 5.836e-3 | 3.785 | 2.529e-3 | 4.040 |
| | 80 | 7.861e-4 | 2.892 | 2.627e-4 | 3.267 |
| | 160 | 3.260e-5 | 4.592 | 7.756e-6 | 5.082 |
| | 320 | 8.444e-7 | 5.271 | 2.055e-7 | 5.238 |
| WENO-5 | 10 | 3.341e-1 | — | 2.100e-1 | — |
| | 20 | 1.070e-1 | 1.643 | 4.896e-2 | 2.101 |
| | 40 | 8.903e-3 | 3.587 | 3.635e-3 | 3.752 |
| | 80 | 1.699e-3 | 2.390 | 4.777e-4 | 2.928 |
| | 160 | 6.813e-5 | 4.640 | 1.482e-5 | 5.011 |
| | 320 | 1.760e-6 | 5.274 | 3.863e-7 | 5.261 |

Table 3: Comparison of convergence and error on $u_t + uu_x = \frac{1}{Re} \frac{\partial^2 u}{\partial x^2}$, with $Re = 1000$.

| Method | N | Convergent Times | $L_\infty error$ | $L_1 error$ |
|--------|----|------------------|------------------|-------------|
| ENN | 40 | 440 | 1.124e-2 | 5.673e-4 |
| | 80 | 843 | 2.219e-2 | 5.671e-4 |
| WENN-5 | 40 | 436 | 1.073e-2 | 5.405e-4 |
| | 80 | 837 | 2.073e-2 | 5.302e-4 |
| WENO-5 | 40 | 440 | 1.112e-2 | 5.623e-4 |
| | 80 | 842 | 2.211e-2 | 5.665e-4 |

(4) Shock-boundary layer interaction

The time-dependent two-dimensional Navier-Stokes equations in Cartesian coordinates have as follows:

$$\frac{\partial U}{\partial t} + \frac{\partial F}{\partial x} + \frac{\partial G}{\partial y} = \frac{\partial F_v}{\partial x} + \frac{\partial G_v}{\partial y} \quad (35)$$

where U is a vector of the conserved variables, F and G are the inviscid fluxes, F_v and G_v are the viscous fluxes.

$$\begin{aligned} U &= (\rho, \rho u, \rho v, \rho e_t)^T \\ F &= (\rho u, \rho u^2 + p, \rho uv, (\rho e_t + p)u)^T \\ G &= (\rho v, \rho uv, \rho v^2 + p, (\rho e_t + p)v)^T \\ F_v &= (0, \tau_{xx}, \tau_{xy}, u\tau_{xx} + v\tau_{xy} + q_x)^T \\ G_v &= (0, \tau_{xy}, \tau_{yy}, u\tau_{xy} + v\tau_{yy} + q_y)^T \\ e_t &= e + \frac{1}{2}(u^2 + v^2) \end{aligned}$$

The shear stresses have the form

$$\begin{aligned} \tau_{xx} &= \frac{\mu}{Re_\infty} \cdot \frac{2}{3}(2u_x - v_y) \\ \tau_{xy} &= \frac{\mu}{Re_\infty} \cdot (u_y + v_x) \\ \tau_{yy} &= \frac{\mu}{Re_\infty} \cdot \frac{2}{3}(2v_y - u_x) \end{aligned}$$

The heat fluxes are

$$\begin{aligned} q_x &= \frac{\mu}{Re_\infty(\gamma - 1)M_\infty^2 Pr} \cdot T_x \\ q_y &= \frac{\mu}{Re_\infty(\gamma - 1)M_\infty^2 Pr} \cdot T_y \end{aligned}$$

The equation of state is

$$T = \frac{\gamma M_\infty^2 P}{\rho}$$

The coefficient of viscosity μ is given by Sutherland's formula:

$$\mu = T^{\frac{3}{2}} \frac{1 + C}{T + C}, C = \frac{110.4}{T_\infty}$$

where Pr is the Prandtl number, M_∞ —the Mach number and Re_∞ —the Reynolds number. In this computation, we introduced a coordinate transformation as follows to satisfy a sufficient number of points within the viscous layer.

$$\begin{cases} \xi = x \\ \eta = 1 - \frac{\ln\left(\frac{\beta + 1 - y_1}{\beta - 1 + y_1}\right)}{\ln\left(\frac{\beta + 1}{\beta - 1}\right)}, \quad y_1 = y/h \end{cases} \quad (36)$$

In this paper, the explicit-implicit method [5] is adopted, i.e. the explicit method is applied in ξ -direction and the implicit method is applied in η -direction.

Computational parameters are

$$\begin{aligned} M_\infty &= 2.0, Re_\infty = 2.96 \times 10^5, T_\infty = 293K \\ \beta &= 1.002, h = 0.1215, \gamma = 1.4, Pr = 0.72 \end{aligned}$$

Following [4], computational domain is chosen to be $0 \leq x \leq 0.32, 0 \leq y \leq 0.1215$, the reference length $L = 0.16$, the impinging shock angle is $\theta = 32.585^\circ$.

Fig.3–fig.6 give the results by using ENN and WENN_5 schemes, fig.3 shows the distributions of pressure and fig.4 shows the distributions of the skin friction coefficient on the wall with 33×33 gridpoints, fig.5 and fig.6 with 65×65 gridpoints.

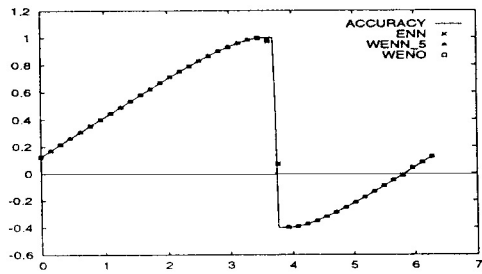


Fig.1 N=40

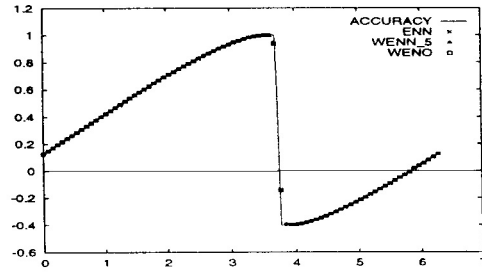


Fig.2 N=80

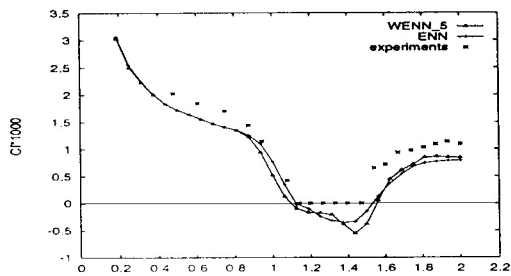


Fig.3 Skin friction distributions on plate

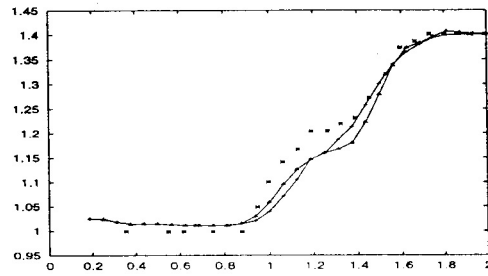


Fig.4 Pressure distributions on plate

Comparison of the ENN and WENN_5 schemes for shock-boundary layer interaction(33x33)

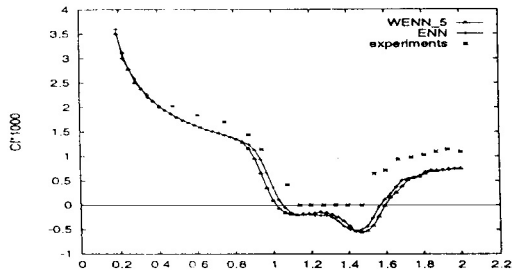


Fig.5 Skin friction distributions on plate

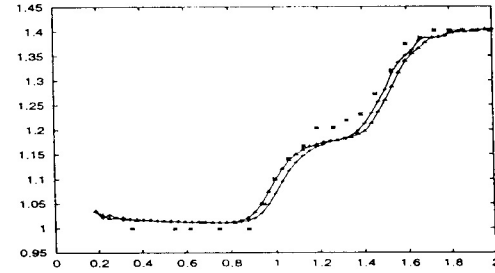


Fig.6 Pressure distributions on plate

Comparison of the ENN and WENN_5 schemes for shock-boundary layer interaction(65x65)

References

- [1] Zhang Hanxin et al., Some important problems for high order accurate difference scheme solving gas dynamic equations, *ACTA Aerodynamica Sinica*, **11**:4 (1993), 347-356.
- [2] Guang-Shan Jiang, Chi-Wang Shu, Efficient implementation of weighted ENO schemes, *J. Comp. phys.*, **126**:1 (1996), 202-228.
- [3] Wang Ruquan , Liu Weiguo, Shen Yiqing, A hybrid high accuracy difference scheme and its applications, *Communications in Nonlinear Science & Numerical Simulation*, **2**:1 (1997), 36-39.
- [4] Z. Wang, B.E. Richards, High resolution schemes for steady flow computation, *J. Comp. Phys.*, **97** (1991), 53-72.
- [5] Yang Dinghui, Comparison study of numerical viscosities of different TVD scheme, M.S. Thesis, The Computing Center, Academia Sinica, 1993.